Time-bin encoding Along Satellite-Ground Channels

Giuseppe Vallone,[1] Daniele Dequal,[1] Marco Tomasin,[1] Francesco Vedovato,[1]
Matteo Schiavon,[1] Vincenza Luceri,[2] Giuseppe Bianco,[3] and Paolo Villoresi[1]

[1]*Dipartimento di Ingegneria dell'Informazione, Università degli Studi di Padova, Padova, Italy.*
[2]*e-GEOS spa, Matera, Italy*
[3]*Matera Laser Ranging Observatory, Agenzia Spaziale Italiana, Matera, Italy*

Introduction - Time-bin encoding is an extensively used technique to encode a qubit in Quantum Key Distribution (QKD) along optical fibers [1–4] and more in general for Quantum Information applications, such as fundamental tests of Quantum Mechanics [5–8], and for increasing the dimension of the Hilbert space in which information can be encoded [9]. Time-bin encoding exploits single photons passing through an unbalanced Mach-Zender interferometer (MZ). The difference in path length must be longer than the coherence length of the photon to avoid first order interference and to have the possibility to distinguish the taken path. If the photon takes the short path, it is said to be in the state $|S\rangle$; if it takes the long path, it is said to be in the state $|L\rangle$. If the photon has a non-zero probability to take either path, then it is in a coherent superposition of the two states:

$$|\psi\rangle = \alpha|S\rangle + \beta|L\rangle\,. \tag{1}$$

In typical QKD experiments, the qubits are encoded in the phase between the two paths with fixed amplitudes, typically at 50%, obtaining

$$|\psi\rangle = \frac{|S\rangle + e^{i\phi}|L\rangle}{\sqrt{2}}. \tag{2}$$

Measurement in the $|S\rangle, |L\rangle$ basis is done by measuring the time of arrival of the photon. Measurement in other bases can be achieved by using a second MZ interferometer before the photon detection, with the same unbalancement of the MZ used on the generation stage.

Despite its success in fibers QKD (in particular in the "plug&play" systems [1]), time-bin encoding was never implemented in long-distance free-space QKD: indeed, turbulence effects on the wavefront are believed to make interference hardly measurable. Here we demonstrate that time-bin interference at the single photon level can be observed along free-space channels and in particular along satellite-ground channels. To this purpose, we used a scheme similar to the "plug&play" systems: a coherent superposition between two wavepackets is generated on ground, sent on space and reflected by a rapidly moving satellite at very large distance with a total path length up to 5000 km. The beam returning on ground is at the single photon level and we measured the interference between the two time-bins. We will demonstrate that the varying relative velocity of the satellite with respect to the ground introduces a modulation in the interference pattern which can be predicted by special relativistic calculations, as explained below. Our results attest the viability of time-bin encoding for Quantum Communications in Space.

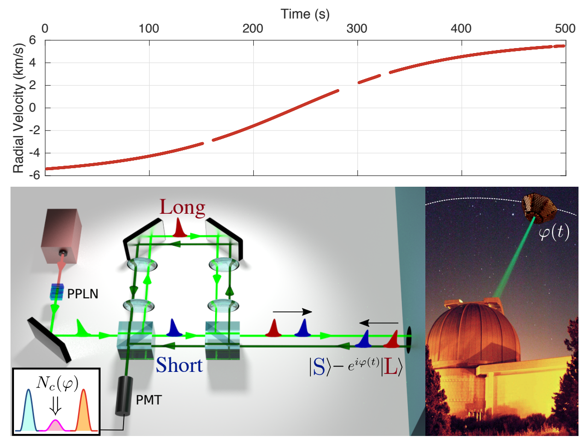

FIG. 1. **Scheme of the experiment and satellite radial velocity**. In the top panel we show the measured radial velocity of the Beacon-C satellite ranging from -6 km/s to $+6$ km/s as a function of time during a single passage. In the bottom panel we show the unbalanced MZI with the two $4f$-systems used for the generation of quantum superposition and the measurement of the interference. Light and dark green lines respectively represent the beams outgoing to and ingoing from the telescope. In the inset, we show the expected detection pattern: the number of counts N_c in the central peak varies according to the kinematic phase φ imposed by the satellite. Right photo shows MLRO with the laser ranging beam and the Beacon-C satellite (not to scale). The phase $\varphi(t)$ depends on the satellite radial velocity as described in the text.

Description of the experiment - In our scheme, a coherent state $|\Psi_{\rm out}\rangle$ in two temporal modes is generated at the ground station with an unbalanced Mach-Zehnder interferometer (MZI), sketched in the lower panel of Fig. 1. The ground station is the Matera Laser Ranging Observatory (MLRO) of the Italian Space Agency in Matera, Italy, that is equipped with a 1.5 m telescope designed for precise satellite tracking and which acted as ground quantum-hub for the first demonstrations of Space Quantum Communication (QC) [10, 11]. The delay $\Delta t \simeq 3.4$ ns between the two time-bins corresponds to a length difference between the two arms of $\ell = c\Delta t \simeq 1$ m (c is the speed of light in vacuum) and it is much longer than the coherence time $\tau_c \approx 83$ ps of each wavepacket. Using the MLRO telescope, the state $|\Psi_{\rm out}\rangle$ is directed towards satellites in a Low Earth Orbit (LEO) equipped with cube-corner retroreflectors (CCR): we selected three LEO satellites – Beacon-C, Stella and Ajisai – for our experiment. Thanks to the CCR properties, the state is automatically redirected toward the ground station, where it is injected into the same MZI used in the uplink. After the reflection by the satellite and the downlink attenuation, the state collected by the telescope has a mean photon number $\mu < 2 \cdot 10^{-3}$ and it can be written as a time-bin qubit $|\Psi_r\rangle = (1/\sqrt{2})(|S\rangle - e^{i\varphi(t)}|L\rangle)$.

The relative phase $\varphi(t)$ is determined by the satellite instantaneous radial velocity with respect to ground, $v_r(t)$. Indeed, at a given instant t, the satellite motion determines a shift $\delta r(t)$ of the reflector radial position, during the separation Δt between the two wavepackets. This shift can be estimated at the first order as $\delta r(t) \approx v_r(t)\Delta t$, and its value may reach a few tens of micrometers for the satellites here used. Therefore, the satellite motion imposes during reflection the additional *kinematic phase* $\varphi(t) \approx 2\delta r(t)(2\pi/\lambda)$ between the wavepackets $|L\rangle$ and $|S\rangle$, where λ is the pulse wavelength in vacuum. By the relativistic calculation detailed in [12], the exact phase imposed by the satellite motion can be evaluated as

$$\varphi(t) = \frac{2\beta(t)}{1+\beta(t)} \frac{2\pi c}{\lambda} \Delta t \tag{3}$$

with $\beta(t) = \frac{v_r(t)}{c}$. We note that the first order approximation of eq. (3) gives the phase $\varphi(t) \approx 4\pi v_r(t)\Delta t/\lambda$ above described. For a typical LEO satellite passage the radial velocity may range from -6 to $+6$ km/s (as shown in in the top panel of Fig. 1 for the selected passage of the Beacon-C satellite), corresponding to a phase range from $-400 rad$ to $+400 rad$.

A single MZI for state generation and detection intrinsically ensures the same unbalance of the arms and avoids active stabilization, necessary otherwise with two independent interferometers. Two $4f$-systems realizing an optical relay equal to the arm length difference were placed in the long arm of the MZI. The relay is required to match the interfering beam wavefronts that are distorted by the passage through atmospheric turbulence: otherwise, the latter may cause distinguishability between the two paths, washing out the interference.

The MZI at the receiver is able to reveal the interference between the two returning wavepackets. At the MZI outputs we expect detection times that follow the well known three-peak profile (see Fig. 1): the first peak represents the pulse $|S\rangle$ taking again the short arm, while the third represents the delayed pulse $|L\rangle$ taking again the long arm. In the central peak we expect indistinguishably between two *alternative possibilities*: the $|S\rangle$ pulse taking the long arm and the $|L\rangle$ pulse taking the short arm in the path along the MZI toward the detector. The signature of interference at the single photon level is then obtained when the counts in the central peak differ from the sum of the counts registered in the lateral peaks. To measure the interference we used a single photon detector (PMT) placed at the available port of the MZI, as shown in Fig. 1. For a moving retroreflector, the probability P_c of detecting the photon in the central peak is given by

$$P_c(t) = \frac{1 - \mathcal{V}(t)\cos\varphi(t)}{2}, \quad \mathcal{V}(t) = e^{-\left(\frac{\Delta t}{\tau_c}\frac{\sqrt{2\pi}\beta(t)}{1+\beta(t)}\right)^2}. \tag{4}$$

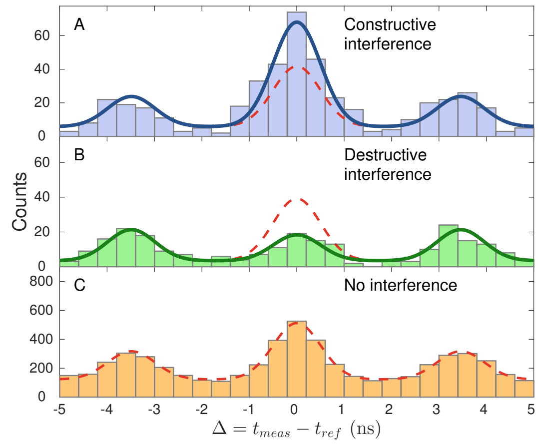

FIG. 2. **Constructive and destructive single photon interference** (Beacon-C satellite, 11.07.2015 h 1.33 CEST). **(A)** Histogram of single photon detections as a function of time $\Delta = t_{meas} - t_{ref}$ realized by selecting only the returns characterized by $\varphi \mod 2\pi \in [4\pi/5, 6\pi/5]$ that lead to constructive interference. Solid line shows the fit. **(B)** Histogram of single photon detections realized by selecting only the returns characterized by $\varphi \mod 2\pi \in [-\pi/5, \pi/5]$. **(C)** Histogram of single photon detections without any selection on the phase. As expected, interference is completed washed out. In all panels, dotted red lines represent the expected counts in case of no interference.

We note that for a retroreflector at rest we expect $P_c = 0$. The above relation is obtained by time-of-flight calculations together with the Doppler effect that changes the angular frequency of the reflected pulses from $\omega_0 \equiv \frac{2\pi c}{\lambda}$ to $\frac{1-\beta}{1+\beta}\omega_0$ (see [12]). The theoretical visibility $\mathcal{V}(t)$ is approximately 1 since the β factor is upper bounded by $3 \cdot 10^{-5}$ in all the experimental studied cases, while $\Delta t/\tau_c$ is of the order of 10^2.

Experimental results - The value of $\varphi(t)$ originating from the satellite motion can be precisely predicted on the base of the sequence of measurements of the instantaneous distance of the satellite, or *range* r, which is realized in parallel. The range is measured by a strong Satellite Laser Ranging (SLR) signal at 10 Hz and energy per pulse of 100 mJ. Then, by measuring the range every 100 ms, the instantaneous satellite velocity relative to the ground station $v_r(t)$ can be estimated, from which $\varphi(t)$ can be derived by Eq. (3). Since $v_r(t)$ is continuously changing along the orbit as shown in Fig. 1 the value of $\varphi(t)$ is varying accordingly.

By the synchronization technique described in detail in [12], we determined of the expected (t_{ref}) and the measured (t_{meas}) instant of arrival of each photon. In this way, the histogram of the detections as a function of the temporal difference $\Delta = t_{\text{meas}} - t_{\text{ref}}$ can be obtained. In Fig. 2 we show such histograms corresponding to constructive and destructive interference in the case of satellite Beacon-C.

In particular, for the constructive interference, Fig. 2A, we selected the detections corresponding to φ (mod 2π) $\in [4\pi/5, 6\pi/5]$. For the destructive interference, Fig. 2B, we selected a kinematic phase φ (mod 2π) $\in [-\pi/5, \pi/5]$. The detections in the central peak are respectively higher or lower

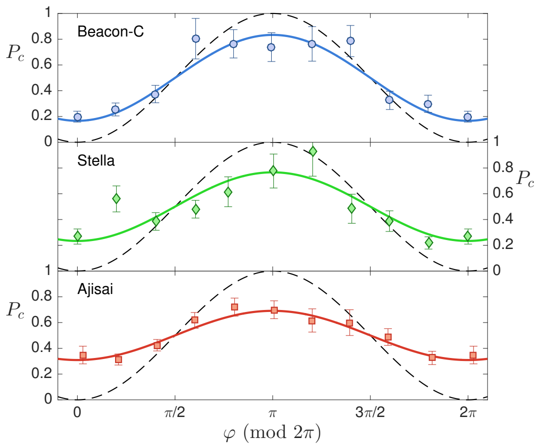

FIG. 3. **Experimental interference pattern**. Experimental probabilities $P_c^{(\rm exp)}$ as a function of the kinematic phase measured for three different satellites. By fitting the data we estimate the visibilities $\mathcal{V}_{\rm exp} = 67 \pm 11\%$ for Beacon-C, $\mathcal{V}_{\rm exp} = 53 \pm 13\%$ for Stella and $\mathcal{V}_{\rm exp} = 38 \pm 4\%$ for Ajisai. Dashed lines correspond to the theoretical value of P_c predicted by eq. (4).

than the sum of the two lateral peaks in the two cases. We note that the peak width is determined by the detector timing jitter which has standard deviation $\sigma = 0.5$ ns. These two histograms clearly show the interference effect in the central peak. On the contrary, Fig. 2C is obtained by taking all the data without any selection on φ. In this case, the interference is completely washed out. These results show that, in order to prove the interference effect, it is crucial to correctly predict the kinematic phase φ imposed by the satellite motion.

By using the data of Fig. 3, we experimentally evaluate the probability $P_c^{(\rm exp)}$ as the ratio of the detections associated the central peak N_c to twice the sum N_ℓ of the detections associated to the side peaks, namely

$$P_c^{(\rm exp)} = \frac{N_c}{2N_\ell} \,. \tag{5}$$

The values $P_c^{(\rm exp)} = 0.87 \pm 0.10$ and $P_c^{(\rm exp)} = 0.20 \pm 0.03$ are obtained for constructive and destructive interference respectively. The values deviates with clear statistical evidence from 0.5, which is the expected value in the case of no interference.

A more clear evidence of the role of $\varphi(t)$ can be demonstrated by evaluating the experimental probabilities $P_c^{(\rm exp)}$ as a function of φ. Fig. 3 shows $P_c^{(\rm exp)}$ for ten different values of the kinematic phase φ and for the three different satellites. By fitting the data by $P_c^{(\rm exp)} = \frac{1}{2}(1 - \mathcal{V}_{\rm exp} \cos\varphi)$, we estimated the experimental visibilities $\mathcal{V}_{\rm exp} = 67 \pm 11\%$ for Beacon-C, $\mathcal{V}_{\rm exp} = 53 \pm 13\%$ for Stella and $\mathcal{V}_{\rm exp} = 38 \pm 4\%$ for Ajisai. The data were collected at the following satellite distance ranges: from 1600 to 2500 km (Ajisai, 12.07.2015, h 3.42 CEST), from 1100 to 1500 km (Stella, 12.07.2015, h 3.08 CEST) and from 1200 to 1500 km (Beacon-C, 11.07.2015, h 1.33 CEST), giving two-way channel lengths ranging from 2200 up to 5000 km. The interference patterns in Fig. 4 clearly demonstrate that the quantum superposition is preserved along these thousand kilometer scale channels with rapidly moving retroreflectors. We attribute the different visibilities to residual vibrations of the unbalanced MZI between the upgoing and downgoing pulses.

Conclusions - Interference between two temporal modes of single photons was observed along a path that includes a rapidly moving retroreflector on a satellite and with length up to 5000 km. We have experimentally demonstrated that the relative motion of the satellite with respect to the ground induces a varying phase that modulates the interference pattern. This varying phase is not present in the case of fixed terminals. The effect resulted from the measured interference pattern during passages of three satellites, Beacon-C, Stella and Ajisai, having different relative velocities and distances from MLRO ground station. We have demonstrated that atmospheric turbulence is not detrimental for time-bin encoding in long distance free-space propagation. Indeed, the two temporal modes separated by a few nanoseconds are identically distorted by the propagation in turbulent air, whose dynamics is in the millisecond scale [13]: the key point here is the careful matching of the interfering wavefronts in the two arms, as shown in Fig. 1. The results here presented attest the feasibility of time-bin/phase encoding technique in the context of Space Quantum Communications.

Furthermore, the measurement of interference in Space is a milestone to investigate the interplay of Quantum Theory with Gravitation. As recently proposed by M. Zych *et al.* [14, 15], single photon interference in Space is a witness of general relativistic effects: gravitational phase shift between a superposition of two photon wavepackets could be highlighted in the context of large distance quantum optics experiment. The interference patterns measured in the present experiment demonstrate that a coherent superposition between two temporal modes holds in the photon propagation and its interference can be indeed observed over very long channels involving moving terminals at fast relative velocity. We believe that the results here described attest the viability of the use of photon temporal modes also for fundamental tests of Physics.

[1] A. Muller, *et al.*, Applied Physics Letters **70**, 793 (1997).
[2] J. Brendel, *et al.*, Phys. Rev. Lett. **82**, 2594 (1999).
[3] N. Gisin, *et al.*, Reviews of Modern Physics **74**, 145 (2002).
[4] V. Scarani, *et al.*, Rev. Mod. Phys. **81**, 1301 (2009).
[5] J. D. Franson, Phys. Rev. Lett. **62**, 2205 (1989).
[6] W. Tittel, *et al.*, Physical Review Letters **81**, 3563 (1998).
[7] G. Lima, *et al.*, Phys. Rev. A **81**, 2 (2010).
[8] G. Carvacho, *et al.*, Phys. Rev. Lett. **115**, 030503 (2015).
[9] I. Ali-Khan, *et al.*, Physical Review Letters **98**, 060503 (2007).
[10] P. Villoresi, *et al.*, New J. Phys. **10**, 033038 (2008), 0803.1871.
[11] G. Vallone, *et al.*, Physical Review Letters **115**, 040502 (2015).
[12] G. Vallone, *et al.*, [arxiv.org:1509.07855] (2015), 1509.07855.
[13] I. Capraro, *et al.*, Phys. Rev. Lett. **109**, 200502 (2012).
[14] M. Zych, *et al.*, Nature Communications **2**, 505 (2011).
[15] D. Rideout, *et al.*, Classical Quant. Grav. **29**, 224011 (2012).